Optical tuning of planar photonic crystals infiltrated with organic molecules

Pascale El-Kallassi,[1,*] Rolando Ferrini,[1] Libero Zuppiroli,[1] Nicolas Le Thomas,[2] Romuald Houdré,[2] Audrey Berrier,[3] Srinivasan Anand,[3] and Anne Talneau[4]

[1]*Laboratoire d'Optoélectronique des Matériaux Moléculaires, Ecole Polytechnique Fédérale de Lausanne (EPFL), CH-1015 Lausanne, Switzerland*
[2]*Institut de Photonique et d'Electronique Quantique, Ecole Polytechnique Fédérale de Lausanne (EPFL), CH-1015 Lausanne, Switzerland*
[3]*Department of Microelectronics and Applied Physics, Royal Institute of Technology (KTH), S-16440 Kista, Sweden*
[4]*CNRS-Laboratoire de Photonique et de Nanostructures (LPN), F-91460 Marcoussis, France*
[*]*Corresponding author: pascale.el-kallassi@epfl.ch*

Received April 18, 2007; accepted May 15, 2007;
posted June 1, 2007 (Doc. ID 82222); published August 7, 2007

The optical tuning of InP-based planar photonic crystals (PhCs) infiltrated with a photoresponsive liquid crystal system is presented. Photoinduced phase transitions of a liquid crystal blend doped with azobenzene molecules are used to tune the optical response of PhC cavities. This process is found to be reversible and stable. Several tuning conditions are analyzed in terms of the blend phase diagram. © 2007 Optical Society of America

OCIS codes: 230.3720, 160.3710, 130.3120, 350.5130, 260.5130.

1. INTRODUCTION

Over the past decade planar photonic crystals (PhCs) consisting of a periodic lattice of low-refractive-index holes in a high-refractive-index dielectric (e.g. semiconductor) matrix have been intensively studied as artificial materials that offer the possibility to control light propagation on the wavelength scale [1]. Using this property, several optical devices based on PhCs have been proposed and experimentally demonstrated in different fields, from quantum optics to integrated optics [1,2]. Recently, increasing attention is being devoted to the necessity of tuning and trimming the optical response of PhC-based devices [1]. This emerging topic may have a strong impact in various application fields, such as integrated optics [1,3], quantum optics [4], detection, and sensing [5]. Among the numerous techniques that have been proposed to tune the optical properties of planar PhCs, infiltrating their holes with an organic material that has a tunable refractive index has proved to be one of the most promising approaches [1]. Several materials have been used and infiltrated in planar PhC structures, such as liquid crystals [6–9], polymers [10], liquids, and liquid dispersions of colloidal quantum dots [11].

In particular, the potential of planar PhC infiltration with nematic liquid crystals (LCs) has been demonstrated [1,6–9]. The molecule shape and alignment are at the origin of the optical anisotropy of a nematic LC that is a birefringent medium with an uniaxial symmetry. When interacting with the nematic LC, light experiences the ordinary refractive index (n_o) or the extraordinary refractive index (n_e) if the electric field is polarized perpendicularly or parallel to the axis of the LC molecule, respectively. The molecular order of a LC can be easily modulated by means of external perturbations, thus providing a change of the LC refractive index on demand. For instance, the optical response of a LC can be tuned by applying an external electric field that modifies the orientation of the molecules with respect to the polarization direction of a light beam propagating through it. Moreover, when the temperature is increased above the nematic–isotropic temperature (clearing point), the molecular order is destroyed and the LC is in its isotropic phase; its optical properties are thus characterized by an isotropic refractive index (n_i) that is independent of the molecule orientation. Both the electric and the temperature tuning mechanisms are reversible, and they have been exploited to tune the optical properties of PhC structures infiltrated with nematic LCs [6–9].

In spite of this large amount of research on LC infiltrated PhCs, little has been done on their optical tuning [12], even though all-optical switching plays a very important role in the optical communication field [13] and several other approaches have already been explored to optically tune planar PhCs [14–18].

In this paper, we show that there is a means of optically tuning the response of planar PhC devices (i.e., simple structures and cavities) by infiltration with a photoresponsive LC system [19–21]. Similar systems have already been used to phototune the optical properties of holographically patterned and polymer-stabilized LC structures [22] and of inverse opals [23]. Here, a photoresponsive mixture of LCs and azobenzene derivatives is used. Photochromic molecules such as azobenzenes can undergo a reversible photochemical reaction (photoi-

somerization) between two molecular forms upon irradiation with UV and visible light. Therefore, when photochromes are dispersed in a nematic LC, photoisomerization of the guest molecules can be used to isothermally induce the nematic–isotropic phase transition of the host LC system [19–21].

Using the technique developed in our previous studies [6], InP-based planar PhCs are infiltrated with a LC photochromic mixture. Optical measurements as a function of temperature and polarization are used to determine the infiltration efficiency [6] and the molecule orientation inside the holes [7]. Thus, the phototuning mechanism is characterized, and the photo and thermal responses of the host–guest blend confined in nanometer-size holes (diameter=200–400 nm) are compared to the behavior of the "bulk" azo-LC system [19,20]. In particular, the spectral response of PhC-based Fabry–Perot (FP) cavities is optically tuned, thus showing the potential of integrating semiconductor-based nanodevices with optically active organic materials.

2. PHOTOCHROMIC LIQUID CRYSTAL MIXTURES

The used photoresponsive LC system consists of nematic LCs[4-cyano-4′-pentylbiphenyl (5CB) from Merck (LC-K15)] as host molecules and 4-butyl-4′-methoxyazobenzene (BMAB) from MDPI as guest molecules [see the chemical structures of the host LC-K15 and the *trans* and *cis* molecular forms of the guest BMAB in Fig. 1(a)]. The clearing point of LC-K15 is T_{NI}(LC-K15)=35°C. For $\lambda \approx 1.5$ μm the ordinary and extraordinary refractive indexes of LC-K15 at $T=24$°C are $n_o=1.501$ and $n_e=1.656$, respectively, while the isotropic refractive index at $T=37$°C is $n_i=1.548$ [24]. BMAB is an azobenzene derivative, and it possesses an alkoxy substituent and a butyl group at the para positions of the azobenzene. BMAB has a liquid crystalline behavior with a nematic–isotropic phase transition temperature at T_{NI}(BMAB)=45°C and a polycrystalline–nematic phase transition temperature at T_{KN}(BMAB)=35°C.

As discussed in Section 1, azobenzene molecules can undergo a reversible photoisomerization between the *trans* (rodlike shape) and the *cis* (bent shape) molecular forms upon irradiation with UV and visible light. In Fig. 1(b), the measured absorption spectra of the *trans* and the *cis* forms of the BMAB molecules are shown. The *trans* isomer has a main absorption band in the UV around 350 nm ($\pi-\pi^*$ molecular transition), whereas the *cis*-isomer has an absorption peak in the visible around 450 nm ($n-\pi^*$ molecular transition). We remark that the absorption band of the host LC-K15 is located in the UV around 280 nm [20] and does not overlap with those of the BMAB. The *trans*-isomer, which is the thermally stable ground state, can transform into the *cis*-isomer by absorbing UV light, and the *cis*-isomer can return to the *trans*-isomer form either by visible light irradiation or by thermal isomerization [25]. The photoisomerization reactions have time scales on the order of picoseconds [25], whereas without illumination, the *cis* form will thermally reconvert to the more stable *trans* form with a lifetime that, for azobenzenes, is typically on the order of hours (the energy barrier for the thermal isomerization is on the order of 90 kJ/mol) [25]. On one hand, upon UV irradiation, a steady state can be reached at which 100% of the *trans* molecules are converted to the *cis* form. On the other hand, since the $n-\pi^*$ band is present in the absorption spectra of both isomers [see Fig. 1(b)], irradiating a photochromic mixture with visible light will bring the system in a photostationary state, whose composition is based on the competition among the photoisomerization rates (in both directions) and the thermal decay rate; thus, a 100%

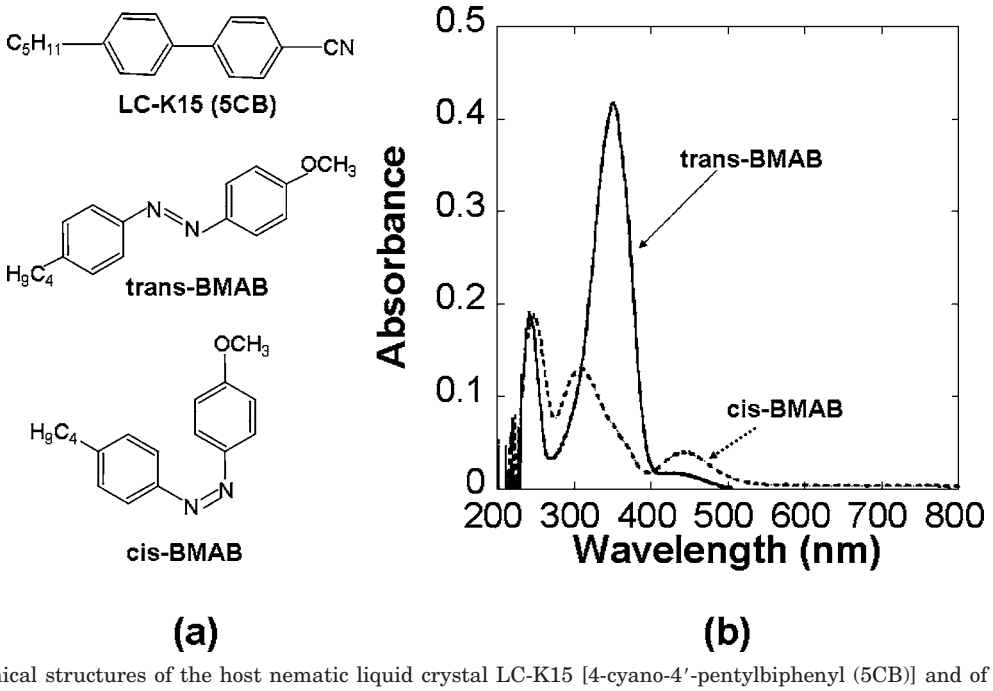

Fig. 1. (a) Chemical structures of the host nematic liquid crystal LC-K15 [4-cyano-4′-pentylbiphenyl (5CB)] and of the *trans* and *cis* molecular forms of the guest azobenzene derivative [4-butyl-4′-methoxyazobenzene (BMAB)]. (b) Measured absorption spectra of the *trans* (full curve) and *cis* (broken curve) forms of the BMAB.

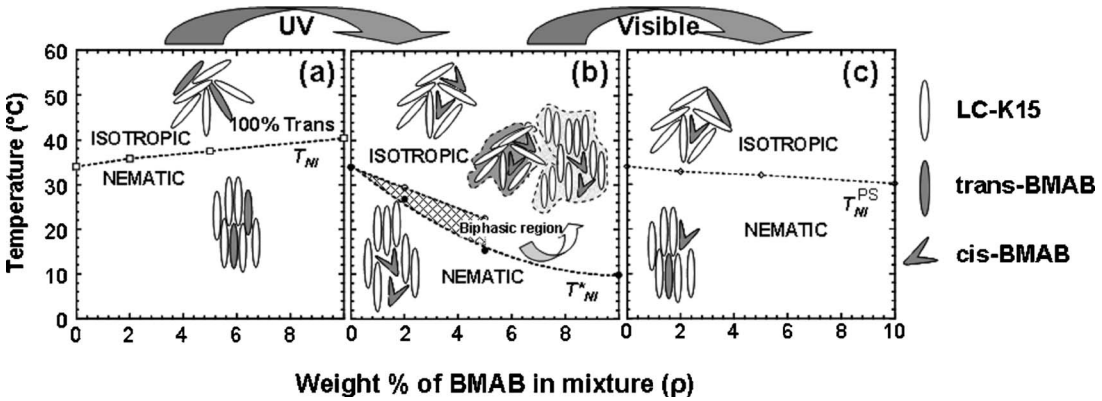

Fig. 2. Phase diagram of the LC-K15/BMAB mixture as a function of the BMAB mole fraction ρ (the values are for the "bulk" azo-LC system and are taken from [20]). The shape of the molecules present in the mixture and the resulting molecular order are sketched. (a) 100% of the BMAB molecules are in the *trans* form, and (b) 100% of the BMAB molecules are in the *cis* form; the shaded region is the biphasic region predicted by the theory of Humphries and Luckhurst [20]. (c) The photostationary state after white light irradiation. T_{NI}, T^*_{NI}, and T_{NI}(PS) are the corresponding nematic–isotropic transition temperatures.

cis-to-*trans* photoconversion is not possible, and the resulting mixture comprises both molecular forms [20].

The phase transitions in a mixture of LC-K15 doped with BMAB are shown in Figs. 2 and 3 as a function of the BMAB mole fraction ρ (the values are for the "bulk" azo-LC system and are taken from [20]). In Fig. 2(a), the nematic–isotropic phase transition temperature T_{NI} is plotted as a function of ρ for a mixture in which all the BMAB molecules are in the *trans* form, i.e., before UV irradiation (the molecular shape and order are sketched in the inset). Owing to its rod-like molecular shape, the *trans* form stabilizes the LC nematic phase, and T_{NI} increases gradually with ρ [20]. Once the mixture is irradiated with UV light and the *trans–cis* photoisomerization takes place, the bent shape of the *cis* isomer introduces molecular disorder in the mixture. Therefore T_{NI} is lowered, and its decrease is proportional to the concentration of the *cis* isomer [20]. In Fig. 2(b), the lowered temperature value T^*_{NI} is plotted as a function of ρ for 100% of the BMAB molecules in the *cis* form. If the system is held at a temperature between T_{NI} and T^*_{NI}, owing to the *trans–cis* photoisomerization of the guest BMAB molecule, the nematic–isotropic phase transition of the LC host can be induced isothermally.

In the equilibrium phase, the BMAB molecules are in the *trans* form, and the system is globally in the nematic phase. Upon irradiation with UV light, the photoisomerization *trans–cis* brings the system into the isotropic phase. A complete photoisomerization is not necessary to induce the nematic–isotropic transition, and response times on the order of milliseconds can be achieved depending on the BMAB concentration, the temperature, and the irradiation power [23]. If the temperature is close to T^*_{NI}, the system may show a biphasic behavior [20]; although no phase separation is observed for mixtures of LC-K15 doped with BMAB, a phase separation between domains of nematic and isotropic LC-K15+*cis* isomers occurs [see Fig. 2(b)]. The photoinduced nematic–isotropic transition is reversible: irradiation with visible light brings part of the *cis* isomers back to the *trans* form and the system back to its nematic phase. This reverse transition has response times on the order of several tens of seconds up to minutes, depending on the temperature and on the percentage of the *cis* isomer in the mixture (i.e., a high concentration of *cis* isomer results in a slower isotropic–nematic transition) [23]. Finally, if the temperature is close to T_{NI}, the system may fall into the photostationary state described above, and the nematic phase cannot be reached simply by visible light irradiation, because the *trans–cis* and *cis–trans* photoisomerization rates are similar. The system is a ternary mixture (LC-K15+*cis* isomers+*trans* isomers), with a nematic–isotropic transition temperature T_{NI}(PS) lower than T_{NI} [see Fig. 2(c)] [20].

The complete phase diagram of the LC-K15/BMAB mixture is summarized in Fig. 3. On one hand, due to the widening of the photostationary region with increasing ρ, the BMAB concentration in the mixture must remain well below 10% if one wants to preserve the complete photoreversibility of the host–guest mixture. For instance, azobenzene-infiltrated inverse opals have been studied, and it has been found that irradiation with visible light cannot regenerate the initial state, which can only be recovered by a thermal process [23]. On the other hand, working conditions close to the photostationary limit may

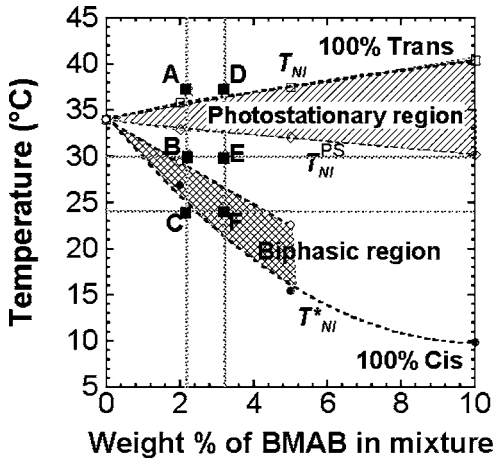

Fig. 3. Complete phase diagram of the LC-K15/BMAB mixture. The photostationary region is hashed. The experimental conditions chosen for the infiltration and the optical tuning of PhCs are indicated (black squares).

shorten the response times of the system [20]. The parameter values (i.e. BMAB concentration and temperature) chosen for the experiments described in Section 5 are reported in Fig. 3 (black squares and letters). Mixtures with $\rho=2.2\%$ and 3.2% were prepared in order to study the influence of the BMAB concentration. The transition temperature T^*_{NI} is expected to be 5°C and 7°C lower than T_{NI} for the 2.2% and 3.2% mixtures, respectively (see Fig. 2). The photostationary state is calculated to be located at about 2°C below T_{NI} [see Figs. 2(b) and 3]. Owing to the low concentration values chosen for the BMAB guest molecules, their influence on the blend refractive index can be considered negligible, and the same values as for pure LC-K15 can be assumed for the n_o, n_e, and n_i refractive indexes of the mixture (see above).

3. InP-BASED PLANAR PHOTONIC CRYSTALS

Planar PhCs consisting of a triangular lattice of air holes were fabricated by electron-beam lithography and chemically assisted ion-beam etching [26] through a nominally undoped InP/(Ga,In)(As,P)/InP vertical waveguide grown by metalorganic vapor-phase epitaxy (see Fig. 4). In the wavelength range of interest (i.e., $\lambda\approx1.5$ μm) the waveguide is single mode for both TE and TM polarization directions (see Fig. 4). At $T=24$°C, the effective refractive indexes are $n_{eff}=3.261$ and 3.252 for the TE and TM guided modes, respectively [7]. Two GaAsInP quantum wells were embedded in the core layer, allowing the internal light source technique to be used to optically characterize the infiltrated PhCs [27]. The photoluminescence excited inside the quantum wells is used as a built-in probe technique. Part of the photoluminescence signal propagates parallel to the surface as a guided mode and interacts with the PhC structure before escaping from a cleaved edge and being spectrally analyzed. The absolute transmission through the PhC structure was obtained by normalizing the spectrum measured after transmission through the PhC with respect to a spectrum collected in a nonpatterned region of the sample. Since internal light source measurements on a single PhC structure yield the transmission spectrum only in a spectral interval of ≈100 nm, the PhCs were replicated with different periods a while keeping the intended air filling factor f value constant (lithographic tuning) [27].

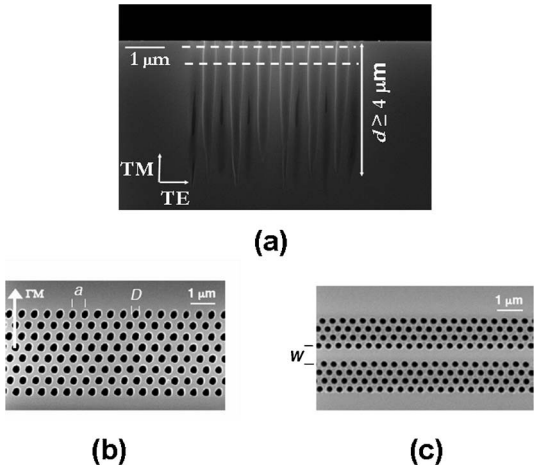

Fig. 4. Scanning electron microscopy. (a) Cut view of a PhC etched through a InP/(Ga,In)(As,P)/InP planar waveguide [the GaInAsP core layer is sketched (dashed lines)]; the hole depth is $d\geq4$ μm. The white arrows indicate the orientation of the electric field for TE and TM polarization directions. (b) Top view of an eight-rows-thick ΓM-oriented PhC slab (a=lattice period, D=hole diameter). (c) Top view of a Fabry–Perot cavity between two four-rows-thick ΓM-oriented PhC mirrors (W=cavity width).

Two types of PhC structures were fabricated with $a=300-600$ nm ($\Delta a=20$ nm): (i) simple eight-row-thick ΓM-oriented PhC slabs and (ii) FP cavities consisting of two four-row-thick ΓM-oriented PhC mirrors separated by a spacer $W/a=1.8$ (see Fig. 4). The filling factor f was measured by fitting the transmission spectra of the empty structures with the finite-difference time domain (FDTD) [27], and the two-dimensional plane wave expansion (PWE) [28] models with f as the only free parameter. We obtain a value $f=0.43\pm0.01$, which corresponds to a hole diameter $D=200-400$ nm.

4. SAMPLE INFILTRATION AND OPTICAL CHARACTERIZATION

The fabricated PhCs were infiltrated with the LC-K15/BMAB mixtures using the vacuum chamber and the infiltration technique described in [6] and specifically developed for the infiltration of planar PhCs. The samples were mounted on a Peltier stage to allow temperature tuning from 20°C up to 40°C. Following the same procedures as those illustrated in [6,7], the transmission through the PhC structures was measured as a function of temperature and polarization in order to determine the infiltration efficiency η and the molecule orientation inside the holes [7]. The experimental measurements were fitted by means of two-dimensional FDTD [27] and PWE [28], with the refractive index value inside the holes n_{hole} as the only free parameter (the slab waveguide effective refractive index n_{eff} was calculated and assumed as the matrix index) [6,7,27].

In particular, the FDTD and PWE fit of the transmission spectra through the simple slabs and the FP cavities at a temperature well above the clearing point of the LC-K15/BMAB mixtures (i.e. $T=37$°C; points A and D in Fig. 3) yield $n_{hole}=1.51\pm0.02$ for both concentrations ρ (see Section 2). The latter values can be translated into an infiltration efficiency $\eta=0.93\pm0.04$ [6]. Once η is deter-

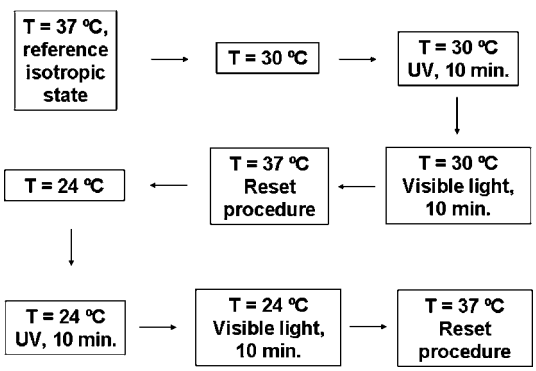

Fig. 5. Irradiation procedure. The transmission through the infiltrated photonic crystals was measured after each step.

mined, n_{hole} can be roughly calculated for the equilibrium molecule configurations inside the holes where the LCs are predominantly oriented either parallel or perpendicularly to the hole axis [7]. For $\eta=0.93\pm0.04$ and a predominant parallel LC orientation, $n_{hole}=1.45$ and 1.63 for the TE and TM polarization directions, respectively. For the chosen concentrations ρ, the fit of the experimental transmission spectra at room temperature (i.e. $T=24°C$; points C and F in Fig. 3) yields $n_{hole}=1.45\pm0.01$ and 1.66 ± 0.01 for the TE and TM polarizations, respectively, thus showing that most of the LC molecules are aligned parallel to the hole axis. More details on the approximations made on the LC refractive index values for different molecule configurations can be found in [7]. We note that the different molecule orientation with respect to [7] may be due to different surface state after PhC etching.

The optical tuning of the infiltrated PhCs was realized using a 6 W UV lamp (by LTF Labortechnik GmbH) emitting at 365 nm (irradiance at the sample=0.1 mW/cm^2) and a 20 W cold light source (by Carl Zeiss AG) emitting in the visible and equipped with a UV filter. The irradiation procedure is described in Fig. 5. The irradiation cycle was repeated several times in order to check the reproducibility of the optical tuning (see Section 5).

5. EXPERIMENTS AND DATA ANALYSIS

In order to illustrate the potential of the LC-K15/BMAB host–guest system for the control of the response of PhC devices, the optical tuning of FP cavities was studied in detail. The phase diagram of the LC-K15/BMAB mixture was explored by measuring the transmission spectra through the infiltrated FP cavities as a function of the temperature T and the BMAB mole fraction ρ (see Fig. 3).

The TE polarized transmission spectra through the FP cavity $W/a=1.8$ ($a=380$ nm) for $\rho=2.2\%$ at temperatures $T=24°C$ and 30°C (points C and B in Fig. 3) are shown in Figs. 6(a) and 6(b), respectively as a function of the energy in reduced units ($u=a/\lambda$). The spectra before and after UV irradiation and after a subsequent irradiation with visible light are reported (gray, dotted and dashed lines, respectively). In both Figs. 6(a) and 6(b), the spectrum measured at $T=37°C$ (thermal isotropic state; point A in Fig. 3) is shown as reference (black solid curve). Before any irradiation, a FP resonance is found at the energy $u_{peak}=0.2455$ and 0.2458 for $T=30°C$ and 24°C, respectively. At $T=37°C$, since $T>T_{NI}$, the LC-15/BMAB mixture is always in the thermal isotropic phase even when 100% of *trans* isomers are present. Thus, the FP resonance redshifts with respect to the lower temperatures (for which $T<T_{NI}$: nematic phase) and is located at $u_{peak}=0.2444$. Light irradiation has no effect at $T=24°C$; since $T<T^*_{NI}$, the system remains in its nematic phase even after a complete photoisomerization, and the shift of the FP resonance after UV irradiation is negligible. At $T=30°C$ ($T^*_{NI}<T<T_{NI}$) after UV irradiation the resonance peak shifts of the same amount as for $T=37°C$; a complete nematic–isotropic phase transition is obtained isothermally by light irradiation (photoisotropic state). Finally, after visible light irradiation the FP peak blueshifts to its original position, thus showing the reversibility of the photoinduced phase transition.

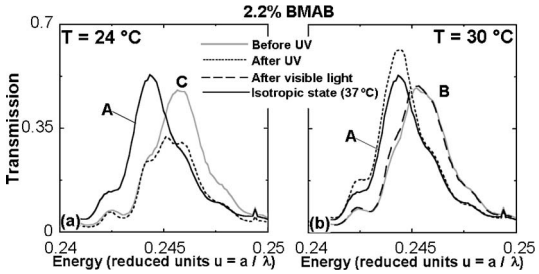

Fig. 6. Measured TE transmission spectra through a Fabry–Perot cavity ($W/a=1.8$, $a=380$ nm) between two four-rows-thick ΓM-oriented PhC mirrors infiltrated with LC-K15/BMAB mixture ($\rho=2.2\%$), before (gray curves) and after irradiation with UV (dotted curves) and visible light (dashed curve), at (a) 24°C and (b) 30°C (corresponding to points C and B in Fig. 3, respectively). The spectrum corresponding to the thermal isotropic state at $T=37°C$ (point A in Fig. 3) is represented as reference (black curve).

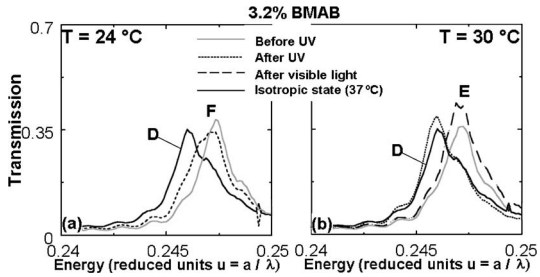

Fig. 7. Measured TE transmission spectra through a Fabry–Perot cavity ($W/a=1.8$, $a=380$ nm) between two four-rows-thick ΓM-oriented PhC mirrors infiltrated with LC-K15/BMAB mixture ($\rho=3.2\%$), before (gray curves) and after irradiation with UV (dotted curves) and visible light (dashed curve), at (a) 24°C and (b) 30°C (corresponding to points F and E in Fig. 3, respectively). The spectrum corresponding to the thermal isotropic state at $T=37°C$ (point D in Fig. 3) is represented as reference (black curve).

The TE polarized transmission spectra through the FP cavity $W/a=1.8$ ($a=380$ nm) for $\rho=3.2\%$ at temperatures $T=24°C$ and 30°C (points F and E in Fig. 3) are shown in Figs. 7(a) and 7(b), respectively. The spectra before and after UV irradiation and after a subsequent irradiation with visible light are reported as in Fig. 6. Before any irradiation, the FP resonance is found at the energy $u_{peak}=0.2472$ and 0.2473 for $T=30°C$ and 24°C, respectively. As for the previous case, in both Figs. 7(a) and 7(b), the spectrum for thermal isotropic state (point D in Fig. 3) is shown as a reference: $u_{peak}=0.2461$. At $T=24°C$ (T in the biphasic region; see Fig. 3), irradiating the sample with UV light does not lead to a complete phase transition; the FP resonance slightly redshifts ($u_{peak}=0.2470$) without joining the peak corresponding to the thermal isotropic state. Owing to the coexistence of both nematic and isotropic domains, for $\rho=3.2\%$ a complete isotropic phase cannot be obtained isothermally by UV irradiation for temperatures below 27°C (see Fig. 3). At $T=30°C$ ($T^*_{NI}<T<T_{NI}$), UV irradiation leads to a complete isothermal transition to the photoisotropic phase; the FP resonance redshifts of the same amount as for $T=37°C$. As in the previous case, the transition can be totally reversed by irradiating the sample with visible light; the FP peak blue-

shifts to its original position, thus showing again the reversibility of the photoinduced phase transition.

The FP peaks were fitted by using an Airy formula [27] and assuming the PhC mirror transmission (T) and reflectivity (R) as free fitting parameters; the values $R=0.88-0.90$ were found for all FP peaks shown in Figs. 6 and 7, which correspond to a cavity quality factor $Q=100-120$. After the photoinduced phase transition, as for the thermal process, R and Q slightly decrease with respect to the nematic state, further confirming the increase of n_{hole}, i.e., the transition to the isotropic phase [6]. Small differences were found in the optical properties of the mirror and cavity for the two concentrations ρ, which is due to the use of two different PhC samples.

Finally, once the isothermal optical tuning was assessed, its reproducibility was successfully verified by repeating UV–visible irradiation cycles and checking that the transmission spectra were always the same after each illumination step (see Fig. 5).

6. CONCLUSION

In conclusion, the optical tuning of planar PhC devices infiltrated with a photoresponsive LC mixture was demonstrated. The phase transition conditions for the host–guest LC-K15/BMAB system were analyzed in detail. BMAB concentrations $\rho \ll 10\%$ were chosen in order to have a fully reversible photoswitchable blend at room temperature. By exploring the complete phase diagram of the LC-K15/BMAB system, the most suitable temperatures for PhC-device operation could be found for each concentration ρ. The photo and thermal response of the infiltrated mixture was found to be the same as in "bulk" azo-LC systems; the confinement of the molecules in nanometer-size holes does not affect the photo switching process.

We note that a phototunable PhC device with good stability and reproducibility has potential applications in several optical devices [14]. Response times on the order of milliseconds to seconds might be achieved, depending on the BMAB concentration, the temperature, and the irradiation power. In spite of their slow response time, PhC devices infiltrated with a photoresponsive LC mixture can be envisaged for reconfiguration applications, switching between different functionalities and adjustment of filter devices [1]. Moreover, the possibility of optically tuning the response of a PhC opens the way to the local tuning of more complex structures. Shining light on a small ensemble of infiltrated holes can modify the optical properties of a whole PhC device [4,11].

ACKNOWLEDGMENTS

The authors thank L. A. Dunbar, M. Longchamp, and M. Schaer from the Ecole Polytechnique Fédérale de Lausanne (EPFL, Switzerland) for their technical help. The PhC samples were fabricated within the framework of the European Network of Excellence on Photonic Integrated Components and Circuits (ePIXnet-contract 004525). This work was performed within the framework of the Swiss National Center of Competence in Research (NCCR) in Quantum Photonics.

REFERENCES

1. K. Busch, S. Lölkes, R. B. Wehrspohn, and H. Föll, *Photonic Crystals* (Wiley-VCH, 2004).
2. J. M. Lourtioz, H. Benisty, V. Berger, J. M. Gérard, D. Maystre, and A. Tchelnokov, *Photonic Crystals* (Springer, 2005).
3. A. Sharkawy, S. Shi, D. W. Prather, S. McBride, and P. Zanzucchi, "Modulating dispersion properties of low index photonic crystal structures using microfluidics," Proc. SPIE **6128**, 61280W-1 (2006).
4. S. Mingaleev, M. Schillinger, D. Hermann, and K. Busch, "Tunable photonic crystal circuits: concepts and designs based on single-pore infiltration," Opt. Lett. **29**, 2858–2860 (2004).
5. M. Lončar, A. Scherer, and Y. Qiu, "Photonic crystal laser sources for chemical detection," Appl. Phys. Lett. **82**, 4648–4650 (2003).
6. J. Martz, R. Ferrini, F. Nüesch, L. Zuppiroli, B. Wild, L. A. Dunbar, R. Houdré, M. Mulot, and S. Anand, "Liquid crystal infiltration of InP-based planar photonic crystals," J. Appl. Phys. **99**, 103105 (2006).
7. R. Ferrini, J. Martz, L. Zuppiroli, B. Wild, V. Zabelin, L. A. Dunbar, R. Houdré, M. Mulot, and S. Anand, "Planar photonic crystals infiltrated with liquid crystals: tuning and optical characterization of molecule orientation," Opt. Lett. **31**, 1238–1240 (2006).
8. B. Maune, M. Lončar, J. Witzens, M. Hochberg, T. Baehr-Jones, D. Psaltis, A. Scherer, and Y. Qiu, "Liquid-crystal electric tuning of a photonic crystal laser," Appl. Phys. Lett. **85**, 360–362 (2004).
9. M. Haurylau, S. P. Anderson, K. L. Marshall, and P. M. Fauchet, "Electrical modulation of silicon-based two-dimensional photonic bandgap structures," Appl. Phys. Lett. **88**, 061103 (2006).
10. R. van der Heijden, C.-F. Carlström, J. Snijders, R. W. van der Heijden, F. Karouta, R. Nötzel, H. Salemink, C. Kjellander, C. Bastiaansen, D. Broer, and E. van der Drift, "InP-based two dimensional photonic crystals filled with polymers," Appl. Phys. Lett. **88**, 161112 (2006).
11. F. Intonti, S. Vignolini, V. Türck, M. Colocci, P. Bettotti, L. Pavesi, S. L. Schweizer, R. Wehrspohn, and D. Wiersma, "Rewritable photonic circuits," Appl. Phys. Lett. **89**, 211117 (2006).
12. B. Maune, J. Witzens, T. Baehr-Jones, M. Kolodrubetz, H. Atwater, A. Scherer, R. Hagen, and Y. Qiu, "Optically triggered Q-switched photonic crystal laser," Opt. Express **13**, 4699–4707 (2005).
13. K. Asakawa, Y. Sugimoto, Y. Watanabe, N. Ozaki, A. Mizutani, Y. Takata, Y. Kitagawa, H. Ishikawa, N. Ikeda, K. Awazu, X. Wang, A. Watanabe, S. Nakamura, S. Ohkouchi, K. Inoue, M. Kristensen, O. Sigmund, P. Ingo Borel, and R. Baets, "Photonic crystal and quantum dot technologies for all-optical switch and logic device," New J. Phys. **8**, 208 (2006).
14. S. H. G. Teo, A. Q. Liu, J. B. Zhang, and M. H. Hong, "Induced free carrier modulation of photonic crystal optical intersection via localized optical absorption effect," Appl. Phys. Lett. **89**, 091910 (2006).
15. X. Hu, Y. Liu, J. Tian, B. Cheng, and D. Zhang, "Ultrafast all-optical switching in two-dimensional organic photonic crystals," Appl. Phys. Lett. **88**, 121102 (2005).
16. F. Raineri, C. Cojocaru, R. Raj, P. Monnier, A. Levenson, C. Seassal, X. Letartre, and P. Viktorovitch, "Tuning a two-dimensional photonic crystal resonance via optical carrier injection," Opt. Lett. **30**, 64–66 (2005).
17. F. C. Ndi, J. Toulouse, T. Hodson, and D. W. Prather, "All-optical switching in silicon photonic crystals waveguides by use of the plasma dispersion effect," Opt. Lett. **30**, 2254–2256 (2005).
18. T. Tanabe, K. Nishiguchi, A. Shinya, E. Kuramochi, H. Inokawa, M. Notomi, K. Yamada, T. Tsuchizawa, T. Watanabe, and H. Fukuda, "Fast all-optical switching using ion-implanted silicon photonic crystal nanocavities," Appl. Phys. Lett. **90**, 031115 (2007).

19. J.-H. Sung, S. Hirano, O. Tsutsumi, A. Kanazawa, T. Shiono, and T. Ikeda, "Dynamics of photochemical phase transition of guest/host liquid crystals with an azobenzene derivative as a photoresponsive chromophore," Chem. Mater. **14**, 385–391 (2002).
20. C. H. Legge and G. R. Mitchell, "Photo-induced phase transitions in azobenzene-doped liquid crystals," J. Phys. D **25**, 492–499 (1992).
21. T. Ikeda, "Photomodulation of liquid crystal orientations for photonic applications," J. Mater. Chem. **13**, 2037–2057 (2003).
22. A. Urbas, V. Tondiglia, L. Natarajan, R. Sutherland, H. Yu, J.-H. Li, and T. Bunning, "Optically switchable liquid crystal photonic structures," J. Am. Chem. Soc. **126**, 13580–13581 (2004).
23. S. Kubo, Z.-Z. Gu, K. Takahashi, A. Fujishima, H. Segawa, and O. Sato, "Control of the optical properties of liquid crystal-infiltrated inverse opal structures using photo irradiation and/or an electric field," Chem. Mater. **17**, 2298–2309 (2005).
24. S. Brugioni, R. Meucci, and S. Faetti, "Refractive indices of liquid crystals E7 and K15 in the mid- and near-IR regions," J. Opt. Technol. **73**, 315–317 (2006).
25. K. G. Yager and C. J. Barrett, "Novel photo-switching using azobenzene functional materials," J. Photochem. Photobiol. A **182**, 250–261 (2006).
26. M. Mulot, R. Ferrini, B. Wild, J. Moosburger, A. Forchel, R. Houdré, and S. Anand, "Fabrication of 2D InP-based photonic crystals by chlorine based chemically assisted ion beam etching," J. Vac. Sci. Technol. B **22**, 707–709 (2004).
27. R. Ferrini, D. Leuenberger, M. Mulot, M. Qiu, J. Moosburger, M. Kamp, A. Forchel, S. Anand, and R. Houdré, "Optical study of two-dimensional InP-based photonic crystals by internal light source technique," IEEE J. Quantum Electron. **38**, 786–799 (2002).
28. M. Plihal and A. A. Maradudin, "Photonic band structure of two-dimensional systems: the triangular lattice," Phys. Rev. B **44**, 8565–8571 (1991).